

Article

Transient Liquid Phase Bonding of Magnesium Alloy AZ31 Using Cu Coatings and Cu Coatings with Sn Interlayers

Abdulaziz Nasser AlHazzaa ^{1,2,*} , Muhammad Ali Shar ², Anas Mahmoud Atieh ³ 
and Hiroshi Nishikawa ⁴

¹ Department of Physics & Astronomy, College of Science, King Saud University, Riyadh 11451, Saudi Arabia

² King Abdullah Institute for Nanotechnology (KAIN), King Saud University, P.O. Box 2455, Riyadh 11451, Saudi Arabia; mashar@ksu.edu.sa

³ Industrial Engineering Department, School of Applied Technical Sciences, German Jordanian University, Amman 11180, Jordan; anas.atieh@gju.edu.jo

⁴ Joining and Welding, Research Institute (JWRI), Osaka University, Osaka 565-0871, Japan; nisikawa@jwri.osaka-u.ac.jp

* Correspondence: aalhazaa@ksu.edu.sa; Tel.: +966-114-697-520

Received: 28 November 2017; Accepted: 11 January 2018; Published: 16 January 2018

Abstract: Transient liquid phase bonding (TLP) of AZ31 samples has been investigated using Cu coatings and Cu coatings with Sn interlayer. Copper coatings were used for one set of the bonds, and a combination of Cu coatings and Sn interlayer was used for the other set of bonds. The bonding temperature was fixed at 520 °C, and various bonding times were applied. This study shows that the bonds produced using only Cu coatings have shown weaker bonds compared to the bonds made using Cu coatings and Sn interlayer. The Cu₂Mg particles were detected at the joint region of both bonds made by Cu coatings and Cu coatings with Sn interlayer by X-ray diffraction (XRD). However, it has been observed that the joint region was dominated by solid solution which is rich in Mg. Sn interlayer was not contributed to the intermetallic compound (IMC) at the joint region, and therefore it was diffused away through the Mg matrix. Within the joint interface, a slight increase of micro-hardness was observed compared to Mg base metal alloy. This was attributed to the formation and presence of IMC's within the joint region. It was noticed that the presence of the Sn interlayer improved the joint strength by reducing the pores at the joint region. Pores were clearly observed for those bonds made using Cu coatings—especially for region where the fracture occurs; this was accomplished by scanning electron microscope (SEM).

Keywords: Mg alloy; coatings; intermetallic compounds (IMCs); diffusion bonding; interlayers

1. Introduction

Recently, there has been a significant increase in demand from the industry for lightweight alloys to be used in a variety of engineering applications. This is mainly because the light materials consume less fuel and therefore reduce both service costs and pollutions. Magnesium and magnesium alloys (especially AZ31) are increasingly used as a replacement of many traditional alloys [1–3]. Magnesium is the lightest industrial metal, about 50% lighter than aluminum. Furthermore, magnesium has excellent damping properties and high specific strength, which increase its use in the automotive industry. There is an increase of the use of magnesium alloys in various applications. Mg AZ31 alloy is increasingly used in the automotive and aerospace industries due to its excellent physical and mechanical properties, which mainly include high specific strength. Therefore, there should be a demand for joining Mg AZ31 parts together. It is known that welding and joining of Mg alloys using

commercial fusion methods such as Tungsten Inert Gas Welding (TIG) and Metal Inert Gas Welding (MIG) have the tendency to create porosities and part distortion at the joint region due to the existence of a stable Mg oxide layer [4]. Therefore, alternative joining techniques have been implemented to achieve solid joints with higher joint strength. One of those alternative techniques is transient liquid phase bonding (TLP), which was widely investigated both theoretically and experimentally for certain similar and dissimilar alloys [5–9]. It was agreed that the choice of the interlayer or coatings is a critical factor in achieving a successful TLP bonding for a certain alloy. The melting of the interlayer/coatings at or below the bonding temperature may result in interruption of the formed oxide layer, and therefore is able to produce metal-to-metal bonding contact. The literature review in this field show that there is a wide application of Al, Ni, and Cu as an interlayer to join Mg AZ31. In case of using Al interlayer, it was found that a brittle intermetallic compound (IMC) $Al_{12}Mg_{17}$ was formed at the joint region for all bonding times tested. Although there was a slight increase in the bonding strength with longer bonding times due to the homogenization of the joint microstructure, grain coarsening played a significant role in reducing the strength of the joint if bonding time exceeded 60 min [10]. In other studies, the effect of bonding time when applying Ni interlayers to join the Mg AZ31 was studied [11]. It was reported that the hardness of the joint increased with the increase of the bonding time due to the growth of Mg-Ni intermetallic compounds. The use of Ni coatings was investigated to bond Mg AZ31 together, where the optimum bonding time was found to be 20 min. However, the IMC Mg_2Ni was detected within the joint region and contributed to the reduction of bond strength [12]. Ni interlayer was also used to join the dissimilar set up of magnesium to aluminum. It was reported that a reaction layer between the two dissimilar materials was formed based on Mg_2Ni , where the fracture occurred within this layer [13].

Cu interlayer was used to bond Mg AZ31 together. It was noticed that the concentration of Cu and the formation of intermetallic compound Mg_2Cu at the joint decreased with increasing bonding time. The optimum bonding time suggested by this study to produce the highest strength of 70.2 MPa was reported to be 30 min [14]. From the scientific literature on TLP bonding of Mg AZ31, it was concluded that one of the major factors that deteriorates the joint strength and the optimized joint is the formation of the IMC compounds at the interface. Nevertheless, using the Cu interlayer, in particular, indicates that the content of intermetallic compounds such as Mg_2Cu were reduced when bonding time increased. Cu coatings with Sn interlayer were successfully used to join Mg AZ31 to Ti-6Al-4V dissimilar alloys [15]. This study found that at the Mg side, the Mg_2Cu was formed where the Sn was diffused away into the Mg and Ti base materials, which was reflected as a diffusion zone by electron probe micro-analysis (EPMA). It was interesting to find that no IMCs were formed at the joint based on Sn-Cu or based on Mg-Sn.

This research study applied Cu coatings to bond AZ31 together in the first approach. In the second approach, a combination of Cu coatings and Sn interlayer were used. The aim of this study is to investigate the effect of combined hybrid Cu coatings with Sn interlayer on the joining of Mg AZ31 and to investigate the formation of IMCs within/at the joint region/interface. Although Cu interlayer was used to bond AZ31 together and a combination of Cu coatings and Sn interlayer was used to bond AZ31 with dissimilar alloy, it was worthwhile to perform a comparable study to investigate if the presence of Sn can improve the joint quality.

2. Experimental Procedure

Magnesium alloy Mg-AZ31 in the form of a cylindrical rod with a diameter of 10 mm was sliced in pieces, where each piece had a thickness of 5 mm. The surfaces of each piece were ground in silicon carbide paper (SiC) down to 1000 grit (1000 particles per square inch) finish to have a uniform surface roughness and mirror-like surface finish. The surfaces were then cleaned by ethanol, flushed with water, dried, and kept in desiccators to be transformed to the coating unit. This research project includes two steps: first vacuum coatings, and followed by TLP bonding.

2.1. Vacuum Coatings of Mg AZ31 by Copper

A Leybold coating system (model UNIVEX 300) (Leybold GmbH, Bayenthal, Germany) was utilized for Cu vacuum coatings inside the vacuum chamber of the coating unit. Copper foil with purity of 99.99% was placed on the resistive tungsten boat. Since the vacuum system uses a turbo molecular pump (Leybold GmbH, Bayenthal, Germany) (TMP), the vacuum reached a value of 1×10^{-6} mbar in a few minutes. At this level of vacuum, the current through the tungsten boat was increased until 44.7 Amps, at which point the liquid Cu starts to evaporate. A coating thickness of 5 μm on the Mg AZ31 surfaces was produced at a coating time of 30 min.

2.2. TLP Bonding of Mg AZ31 Using Cu Coatings and Cu Coatings with Sn Interlayer

Based on the scientific literature, it was reported that a bonding time of 30 min was the optimum bonding time to bond Mg-AZ31 together using Cu interlayer. In this study, we tested two scenarios for the interlayers used between the similar Mg-AZ31 alloy; the first is the Cu coatings only, and the second is the Cu coatings with a Sn interlayer.

For the first scenario we selected two bonding times of 10 and 30 min. In the second scenario—which involves 50-micron Sn foil—we have tested bonding times of 10, 20, 30, 40, and 50 min. The bonding temperature was set to 520 °C, and it was fixed for all bonding experiments. A uniaxial pressure of 0.5 MPa was applied in order to enhance the surface-to-surface contact during the TLP bonding. Argon gas (Nippon Tokusyu Kikai Co., Osaka, Japan) was used to shield the samples from contamination and oxidation during the bonding experiments. A high heating rate ramp was applied where the heating temperature reached 520 °C in about 2 min. The schematics of the thermo-compression bonding and the temperature profile are illustrated in Figure 1. When the bonding time was completed for each sample, it was lifted to cool down to ambient temperature, and then it was taken out from the chamber. The bonded sample was cut across the joint in a perpendicular fashion and then mounted in Bakelite powder (Buehler, Lake Bluff, IL, USA). Each bonding experiment was repeated twice to use one of them for shear testing, and to confirm reproducibility. The bonded samples which were mounted in Bakelite were ground and polished in an aluminum oxide suspension (Buehler, Lake Bluff, IL, USA) down to 1 μm for metallurgical observations. A JSM-7600F scanning electron microscope (SEM) (Joel, Tokyo, Japan) was used to study and characterize the microstructure of the joints. X'Pert Pro X-ray diffraction equipment (PANalytical, Almelo, Netherlands) was used to study the fractured surfaces and identify the IMCs. The micro-hardness profiles of the joints were examined using a Vickers Hardness (Buehler's 5100 series micromet) (Buehler, Lake Bluff, IL, USA) with a load of 1000 g and a dwell time of 15 s. The shear strength of the joints was measured by a Tinius Olsen shear tester as described in ASTM-D1002 (ASTM D1002-10, Tinius Olsen TMC, Horsham, PA, USA, 1999).

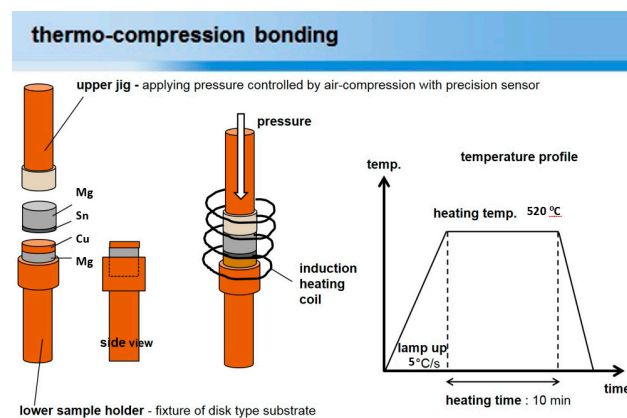


Figure 1. Schematics of the thermo-compression bonding and temperature profile.

3. Results and Discussion

3.1. Analyzing the Joint Region

Figure 2 shows the joint regions of the bond made using Cu coatings for 10 and 30 min bonding times. At a bonding time of 10 min it was observed that a layer of about 70 μm thickness was formed at the joint region due to eutectic reaction between Mg and Cu, noting that the bonding temperature is over the eutectic temperature of the Cu-Mg system. As the bonding time increased to 30 min, a layer of about 50 μm was present at the joint region. This layer originated from the eutectic reaction between Mg and Cu that starts to form at 485 $^{\circ}\text{C}$ based on the binary phase diagram. This layer is attributed to the diffusion of Mg into the joint region that is initially dominated by Cu coatings. Since Mg diffusion into Cu is much higher than the Cu diffusion into Mg, pores were clearly observed between the formed layer and the base material, as shown in Figure 2b.

These results agreed with the observation of bonding Mg AZ31 alloy using Cu interlayer [14,16]. For bonds made at 30 min it can be noticed that there is a distinctive layer at the joint region as provided by SEM micrographs. This means that if bonding time was increased, the layer caused by the eutectic reaction between Mg and Cu would still exist. Figure 3 shows another SEM micrograph for the bond made at 30 min in SEI mode with its corresponding EDS analysis (Joel, Tokyo, Japan). The EDS analysis shows that the weight percent of the Mg, Al, and Cu present at the joint region were 87, 8, and 3 weight percent (wt. %), respectively. These values reflect the fact that Cu dissolution through the base material and the diffusion of Mg and its alloys were rapid and dominated the joint region. The diffusion coefficient of Mg into Cu is $2 \times 10^{-13} \text{ cm}^2/\text{s}$, whereas the diffusion coefficient of Cu in Mg is $5.8 \times 10^{-14} \text{ cm}^2/\text{s}$ at 500 $^{\circ}\text{C}$ [17–19]. Therefore, the diffusion of Mg into the joint region is significant and plays an important role in the mechanism of bonding formation. It is expected that the layer formed consists of Mg solid solution and IMCs based on the eutectic reaction.

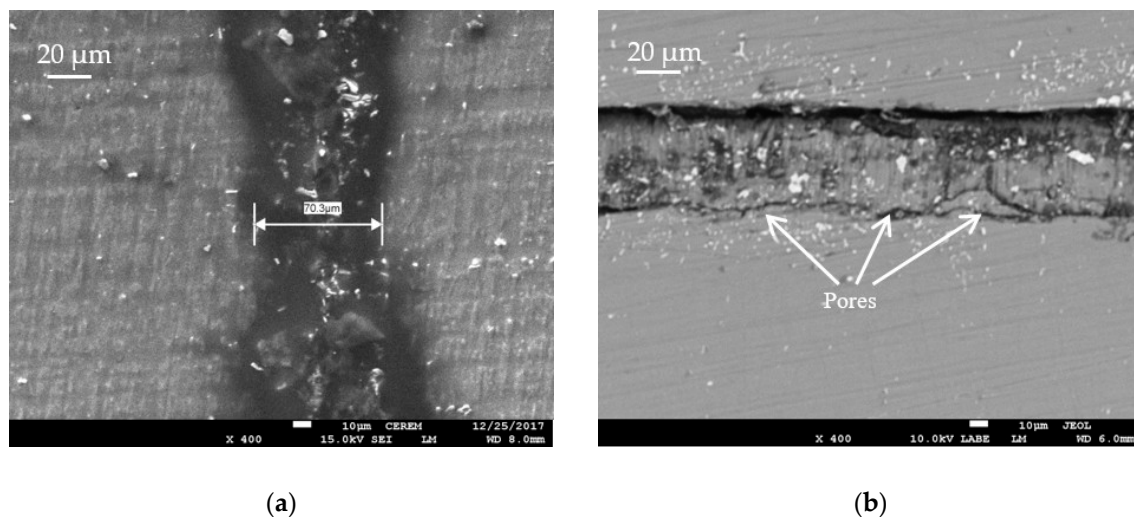


Figure 2. Scanning Electron Microscope Backscattered images of the joints using Cu coating for bond made at (a) 10 min and (b) 30 min.

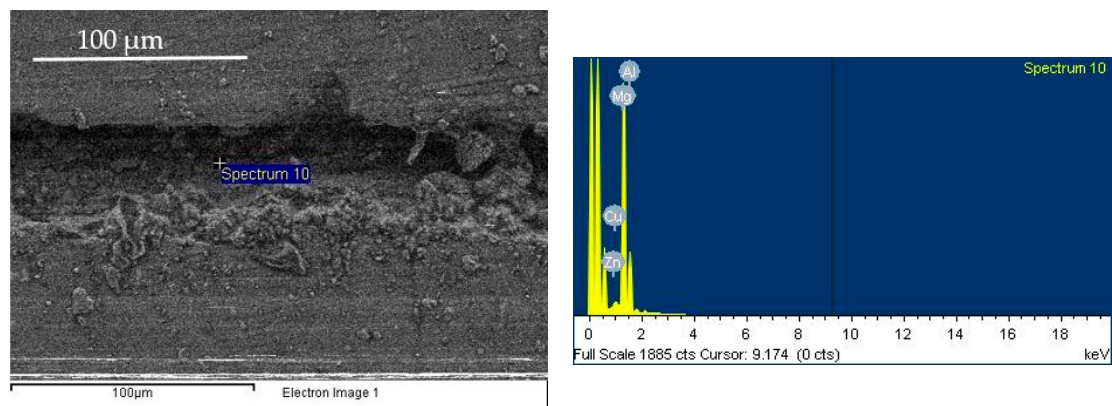


Figure 3. Scanning Electron Microscope (SEM) micrograph of the joint using Cu coating for bond made at 30 min and its corresponding Energy Dispersive Spectroscopy (EDS) analysis.

Bonds made using copper coatings and Sn interlayer were analyzed by SEM and EDS. It was observed that Sn-rich regions were present at the joint interface for bonds made at bonding times of 10 and 20 min, as seen in Figure 4a,b. On the other hand, as bonding time increased, the Sn-rich regions seemed to disappear from the joint as seen in the SEM images. Figure 4c,d show the joint region for bonds made at 30 and 50 min. It was expected that the Sn interlayer which melts at 230 °C dissolved the Cu coatings and diffused away through the base alloy. Mg is also expected to diffuse into the joint region to form a solid solution. Figure 5 shows the EDS analysis of the joint region for bonds made using Cu coating and Sn interlayer at 30 min. The weight percentages of the elements presented at the joint region were measured by EDS. The weight percentages of Mg, Al, Zn, Cu, and Sn were 92.8, 4.6, 0.85, 0.8, and 1.7 wt. % respectively. This shows that the joint region contains a solid solution of Mg due to the diffusion of Sn and Cu into Mg alloy and the diffusion of Mg into the joint region which consists of liquid Sn with dissolved Cu. The presence of IMCs at the joint region is discussed in the later section utilizing the X-ray diffraction.

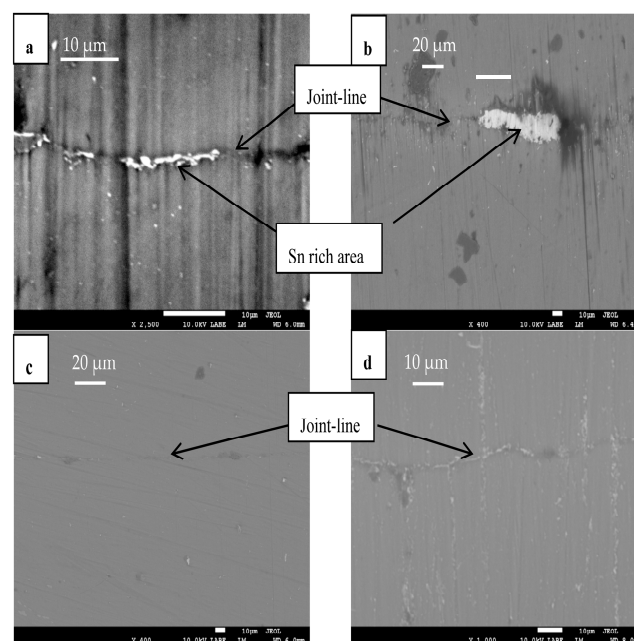


Figure 4. SEM backscattered images for bonds made using Cu coating and Sn interlayer at (a) 10 min; (b) 20 min; (c) 30 min; and (d) 50 min.

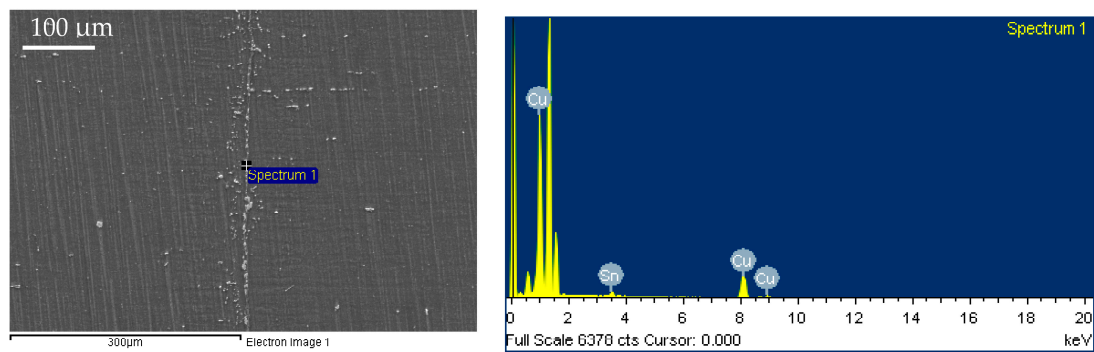


Figure 5. SEM micrograph of the joint using Cu coating and Sn interlayer for a bond made at 30 min and its corresponding EDS analysis.

Although the joint line for a bond made at 30 min using Cu coating and Sn interlayer did not show a distinctive layer, some parts of the joint line appeared to have features which could indicate the formation of IMCs. For that reason, further investigation by EPMA analysis was undertaken. Figure 6 shows high-magnification EPMA analysis for Mg and Cu for a selective area at the joint region. This selective area indicated that there is the presence of Cu and Mg without any indication of the presence of Sn.

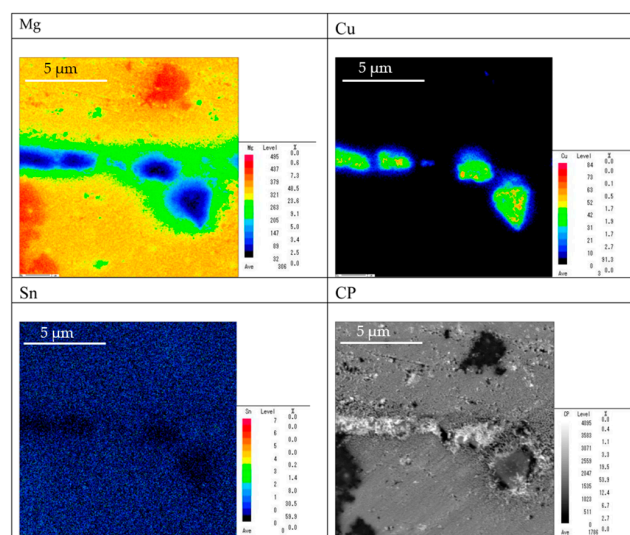


Figure 6. Electron probe micro-analysis (EPMA) images of Mg, Cu, and Sn for bonds made using Cu coating and Sn interlayer at 30 min.

3.2. Micro-Hardness and Shear Tests

The micro-hardness profiles for each bond were measured within 200 microns away from the joint center. A common observation was seen for each bond, that the micro-hardness of the joint was slightly higher than the micro-hardness of the base materials. This can be shown in Figure 7 for the micro-hardness profile for bonds made at 30 and 50 min using Cu coating and Sn interlayer and the bond made at 30 min using Cu coating. The micro-hardness at the joint region was measured as 68, 70, and 65 VHN for bonds made at 30 min and 50 min using Cu coating and Sn interlayer and 30 min using only Cu coating, respectively. The micro-hardness values at 200 µm away from the center of the joint region for each bond were almost identical, at around 58 VHN. The increase in microhardness at the joint region could be due to the presence of IMCs. The shear strength was measured for each bond as a function of bonding time, as seen in Figure 8. It was observed that the shear strength increased with the increase of bonding time and reached 41 MPa for the bond made at 30 min using Cu coatings

and 67 MPa for the bond made at 50 min using Cu coating and Sn interlayer. The latter strength value represents 79% of the strength of the base alloy of Mg AZ31 [20]. The shear strength of the bonds made using Cu coating and Sn interlayer was observed to be drastically increasing with bonding time until 30 min. After that, the increase of the shear strength was not significant. There was a significant difference between the strength of the bond using Cu coating only and Cu coating with Sn interlayer at the same bonding time. For example, the shear strength of the bond made using Cu coating at 30 min was measured to be 41 MPa, whereas it was measured to be 64 MPa for the bond made using Cu coating and Sn interlayer. This significant difference in the strength in favor of using Cu coating and Sn interlayer could be speculated to be either due to the difference in the IMC formation at the joint which weakened the bond made using Cu coatings, or due to the formation of porosities for the bond made using Cu coating. The results obtained by micro-hardness profiles suggested that both Cu coating and Cu coating with Sn interlayer bonds formed IMCs with no significant difference. Therefore, the formation of porosities and the presence of macroscopic vacancies might be responsible for easing the fracture propagation and weakening the bonds made only by Cu coatings.

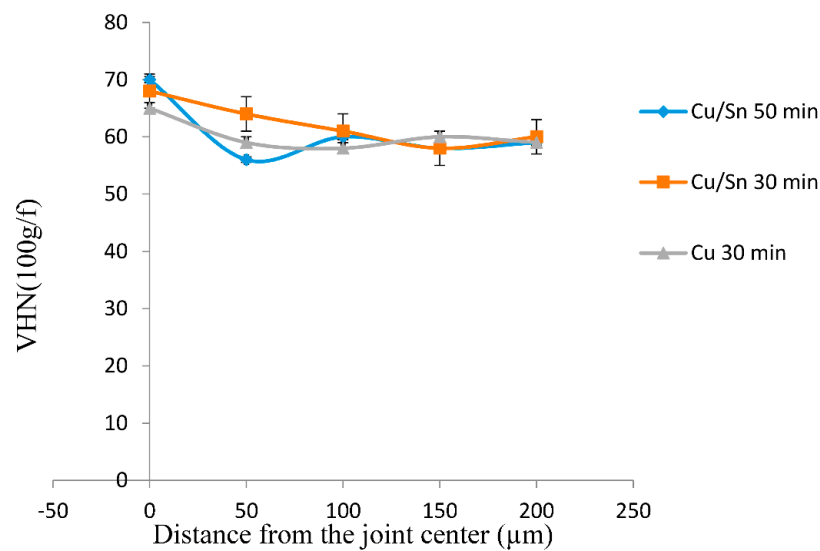


Figure 7. Micro-hardness profiles across the joints as a function of bonding time.

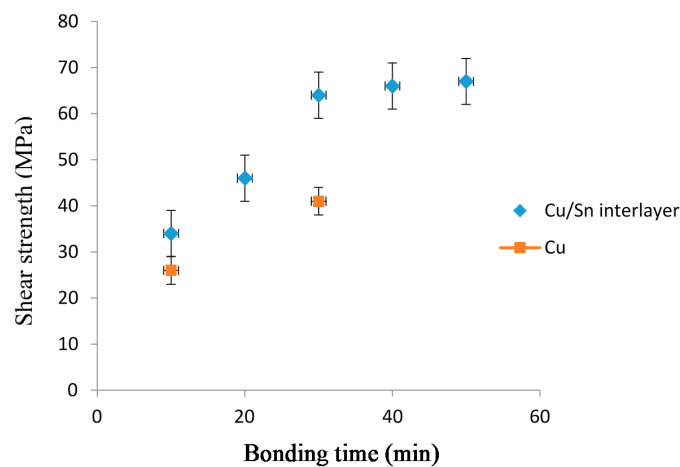


Figure 8. Shear strength of the bonds as a function of bonding time.

3.3. Analysis of the Fractured Surfaces

In order to understand the mechanism of the fracture and the cause of the weak joints (especially for bonds made using only Cu coatings), SEM images of the fractured surfaces were taken as shown in Figure 9. For bonds made using Cu coatings, the fractured surfaces contained porosities which suggests that the fracture occurred through those pores as a result of the difference in the diffusion rate between Mg and Cu Mg-Cu. The presence of these pores was also seen in Figure 2b. On the other hand, there was no indication of porosities at the fractured surface for the bond made using Cu coating and Sn interlayer (see Figure 9b), where a surface with brittle-like structure was observed. Tin (Sn) that melts at a temperature much lower than the bonding temperature is expected to wet the interface and prevent the formation of pores which could form as a result of diffusion. The fractured surfaces were analyzed by XRD, as seen in Figures 10 and 11. The XRD analysis reveals that the microstructure of the fractured surfaces and therefore the microstructure of the joint regions consist of magnesium solid solution and Cu_2Mg compounds (JCPDS file No. 00-035-0821, 03-065-5831). There was no evidence of the presence of any other compounds based on Mg-Sn or Cu-Sn for the fractured surfaces of bonds made using Cu coating and Sn interlayer as seen in Figure 11. Although there is no complete constitution diagram available for the Mg-Cu-Sn system, the detection of Cu_2Mg compound agreed with a previous study that suggested an increase of the stability of the Cu_2Mg phase with the presence of Sn [21].

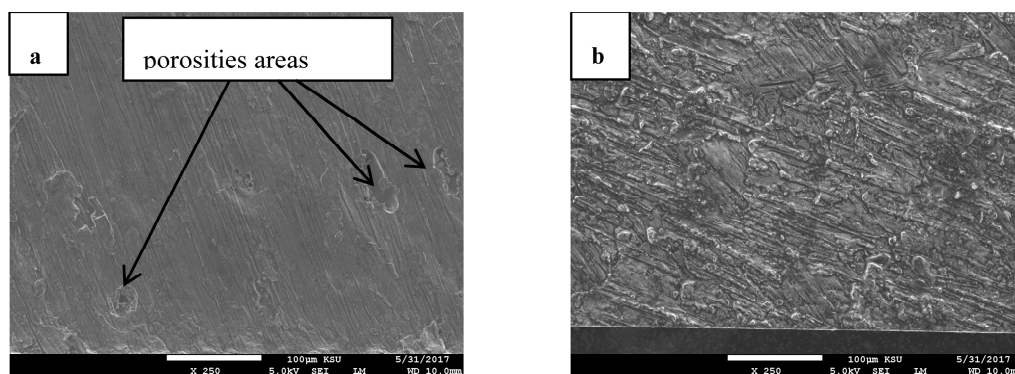


Figure 9. Fractured surfaces of the bonds made at 30 min made by (a) Cu coatings (b) Cu coating and Sn interlayer.

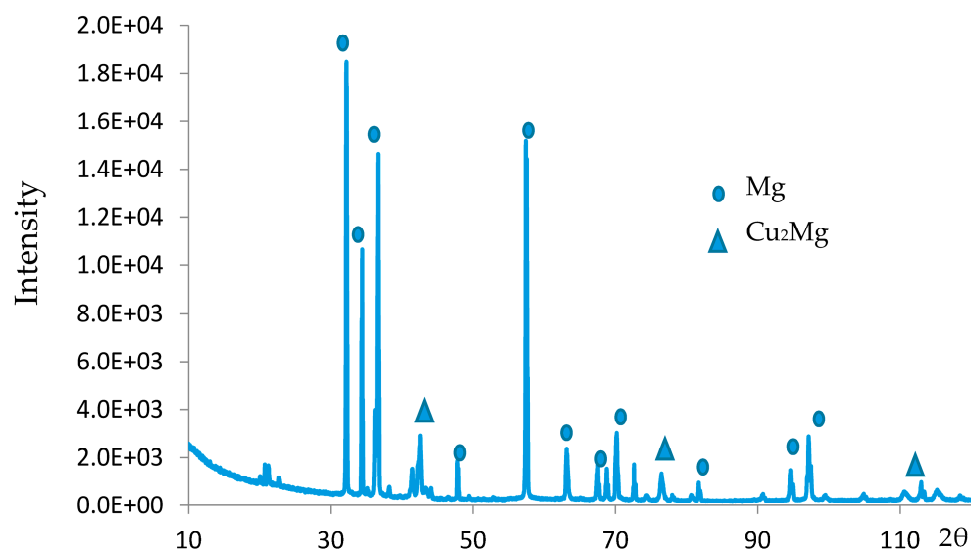


Figure 10. X-ray diffraction (XRD) pattern for bond made using Cu coatings at 30 min.

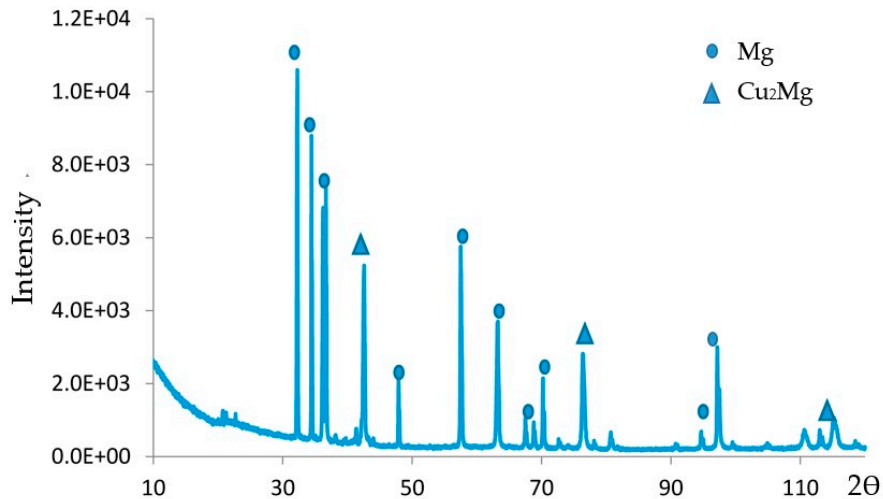


Figure 11. XRD pattern for bond made using Cu coatings and Sn interlayer at 30 min.

4. Conclusions

Identical Mg-AZ31 alloy was successfully bonded together using TLP bonding utilizing two interlayers of Cu coatings and hybrid Cu coatings with the assistance of Sn foil interlayer. The study shows that using Cu coatings with Sn interlayer may produce better joint with higher shear strength due to the absence of porosities at the joint interface. The bonds made using Cu coatings showed a distinctive layer at the joint that consists of Mg solid solution and Cu₂Mg compound with some porosities. Bonds made using Cu coatings and Sn interlayer showed a more homogenized joint region with the increase of bonding time. The shear strength of the joint increased with the increase of bonding time, but the increase in strength beyond 30 min bonding time was not significant. This study shows that there was no formation of IMCs based on Sn-Cu or Mg-Sn at the joint region where only Cu₂Mg compound was detected by XRD. The fracture occurred within the porosities for the bond made using Cu coatings, whereas the fracture occurred within the joint region which contains Mg solid solution and Cu₂Mg compounds for the bonds made using Cu coatings and Sn interlayer. Besides Cu coatings, the use of Sn interlayer resulted in an improvement to the joining quality by reducing the porosities at the joint region. In addition, Sn did not form IMCs with either Mg or Cu, which might result in a weakening of the bonds. Therefore, the use of a hybrid combination of Cu coatings and Sn interlayer produced better bonds compared to Cu coatings alone.

Acknowledgments: The authors extend their appreciation to the Deanship of Scientific Research at King Saud University for funding this work through the Research Project No. NFG-14-03-27.

Author Contributions: The experiments were designed by Abdulaziz Nasser AlHazaa and Anas Mahmoud Atieh. Muhammad Ali Shar, Hiroshi Nishikawa and Abdulaziz Nasser AlHazaa carried out the experiments. Results and data were analyzed by Abdulaziz Nasser AlHazaa and Anas Mahmoud Atieh. The manuscript was written by Abdulaziz Nasser AlHazaa and revised by Anas Mahmou Atieh and Hiroshi Nishikawa.

Conflicts of Interest: The authors declare no conflict of interest.

References

- Westengen, H.; Rashed, H.M.M.A. Magnesium Alloys: Properties and Applications. In *Reference Module in Materials Science and Materials Engineering*; Elsevier: Amsterdam, The Netherlands, 2016.
- Luo, A.A. Magnesium: Current and potential automotive applications. *J. Miner. Met. Mater. Soc.* **2002**, *54*, 42–48. [[CrossRef](#)]
- Mordike, B.L.; Ebert, T. Magnesium, properties–applications–potential. *Mater. Sci. Eng. A* **2001**, *302*, 37–45. [[CrossRef](#)]
- Czerwinski, F. *Magnesium Injection Molding*; Springer: New York, NY, USA, 2008.

5. Isaac Tuah-Poku, M.; Dollars, T.B.M. A study of the transient liquid phase bonding process applied to Ag/Cu/Ag Sandwich joint. *Metall. Trans. A* **1988**, *19*, 675–686. [[CrossRef](#)]
6. Shrzadi, A.A.; Wallach, E.R. Analytical modeling of transient liquid phase (TLP) diffusion bonding when a temperature gradient is imposed. *Acta Mater.* **1999**, *47*, 3551–3560. [[CrossRef](#)]
7. Zhou, Y.; Gale, W.F.; North, T.H. Modeling of transient liquid phase bonding. *Int. Mater. Rev.* **1995**, *40*, 181–196. [[CrossRef](#)]
8. Illingworth, T.C.; Golosnoy, I.O.; Clyne, T.W. Modelling of transient liquid phase bonding in binary systems—A new parametric study. *Mater. Sci. Eng. A* **2007**, *445–446*, 493–500. [[CrossRef](#)]
9. Padron, T.; Khan, T.I.; Kabir, M.J. Modelling the transient liquid phase bonding behavior of a duplex stainless steel using copper interlayers. *Mater. Sci. Eng. A* **2004**, *385*, 220–228. [[CrossRef](#)]
10. Sun, D.Q.; Gu, X.Y.; Liu, W.H. Transient liquid phase bonding of magnesium alloy (Mg–3Al–1Zn) using aluminum interlayer. *Mater. Sci. Eng. A* **2005**, *391*, 29–33. [[CrossRef](#)]
11. Jin, Y.J.; Khan, T.I. Effect of bonding time on microstructure and mechanical properties of transient liquid phase bonded magnesium AZ31 alloy. *Mater. Des.* **2012**, *38*, 32–37. [[CrossRef](#)]
12. AlHazaa, A.N.; Khalil, K.A.; Shar, M.A. Transient liquid phase bonding of magnesium alloys AZ31 using nickel coatings and high frequency induction heat sintering. *J. King Saud Univ. Sci.* **2016**, *28*, 152–159. [[CrossRef](#)]
13. Zhang, J.; Luo, G.; Wang, Y.; Shen, Q.; Zhang, L. An investigation on diffusion bonding of aluminum and magnesium using a Ni interlayer. *Mater. Lett.* **2012**, *83*, 189–191. [[CrossRef](#)]
14. Sun, D.Q.; Liu, W.H.; Gu, X.Y. Transient liquid phase bonding of magnesium alloy (Mg–3Al–1Zn) using copper interlayer. *Mater. Sci. Technol.* **2004**, *20*, 1595–1598. [[CrossRef](#)]
15. AlHazaa, A.N. Effect of Bonding Temperature on the Microstructure and Strength of the Joint between Magnesium AZ31 and Ti–6Al–4V Alloys Using Copper Coatings and Tin Interlayers. *Key Eng. Mater.* **2017**, *735*, 34–41. [[CrossRef](#)]
16. Atieh, A.M.; Khan, T.I. Transient liquid phase (TLP) brazing of Mg–AZ31 and Ti–6Al–4V using Ni and Cu sandwich foils. *Sci. Technol. Weld. Join.* **2014**, *19*, 333–342. [[CrossRef](#)]
17. Zhou, B.-C.; Shang, S.-L.; Wang, Y.; Liu, Z.-K. Data set for diffusion coefficients of alloying elements in dilute Mg alloys from first-principles. *Data Brief* **2015**, *5*, 900–912. [[CrossRef](#)] [[PubMed](#)]
18. Dai, J.; Jiang, B.J. The solidification of multicomponent alloys. *Phase Equilib. Diffus.* **2015**, *36*, 4–18.
19. Combronde, J.; Brebec, G. Diffusion of Ag, Cd, In, Sn and Sb in magnesium. *Acta Metall.* **1972**, *20*, 37–44. [[CrossRef](#)]
20. Campanella, L.C.; Suhuddinb, U.F.H.; Antoniallia, A.Í.S.; dos Santosb, J.F.; de Alcântaraa, N.G.; Bolfarini, C. Metallurgy and mechanical performance of AZ31 magnesium alloy friction spot welds. *J. Mater. Process. Technol.* **2013**, *213*, 515–521. [[CrossRef](#)]
21. Predel, B.; Ruge, H. Study of the Enthalpies of Formation in the Mg–Cu–Zn, Mg–Cu–Al and Mg–Cu–Sn Systems as a Contribution to the Understanding of the Binding Conditions of Laves Phases. *Mater. Sci. Eng.* **1972**, *9*, 141–151. [[CrossRef](#)]

